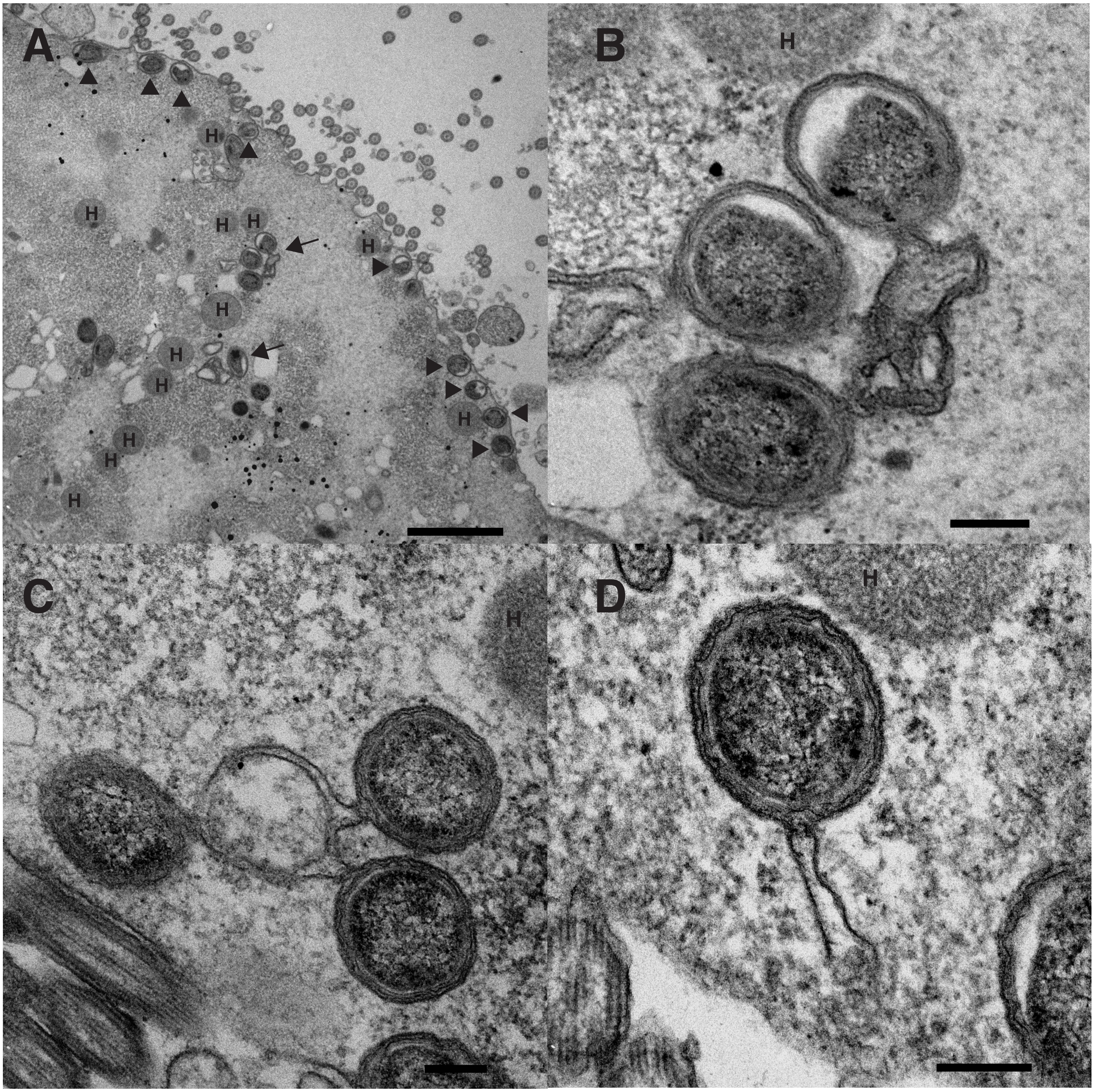

Supplementary Figure S1. Transmission electron microscopy of '*Candidatus* Desulfovibrio trichonymphae' cells hosted by *Trichonympha agilis* cells. (A) '*Ca*. Desulfovibrio trichonymphae' cells in a *T. agilis* cell. Arrowheads indicate '*Ca*. Desulfovibrio trichonymphae' cells proximal to the host cell surface, and arrows indicate those deep inside the *T. agilis* cell. H: hydrogenosome. (B) Magnified image of the '*Ca*. Desulfovibrio trichonymphae' cells indicated by an arrow in panel A. The cells were connected to each other by host-derived tube-like structures. (C) Another example of '*Ca*. Desulfovibrio trichonymphae' cells connected by tube-like structures in a *T. agilis* cell. (D) A '*Ca*. Desulfovibrio trichonymphae' cell with an extended tube-like structure in a *T. agilis* cell. Bars: 2 µm (A); 200 nm (B, C, and D).

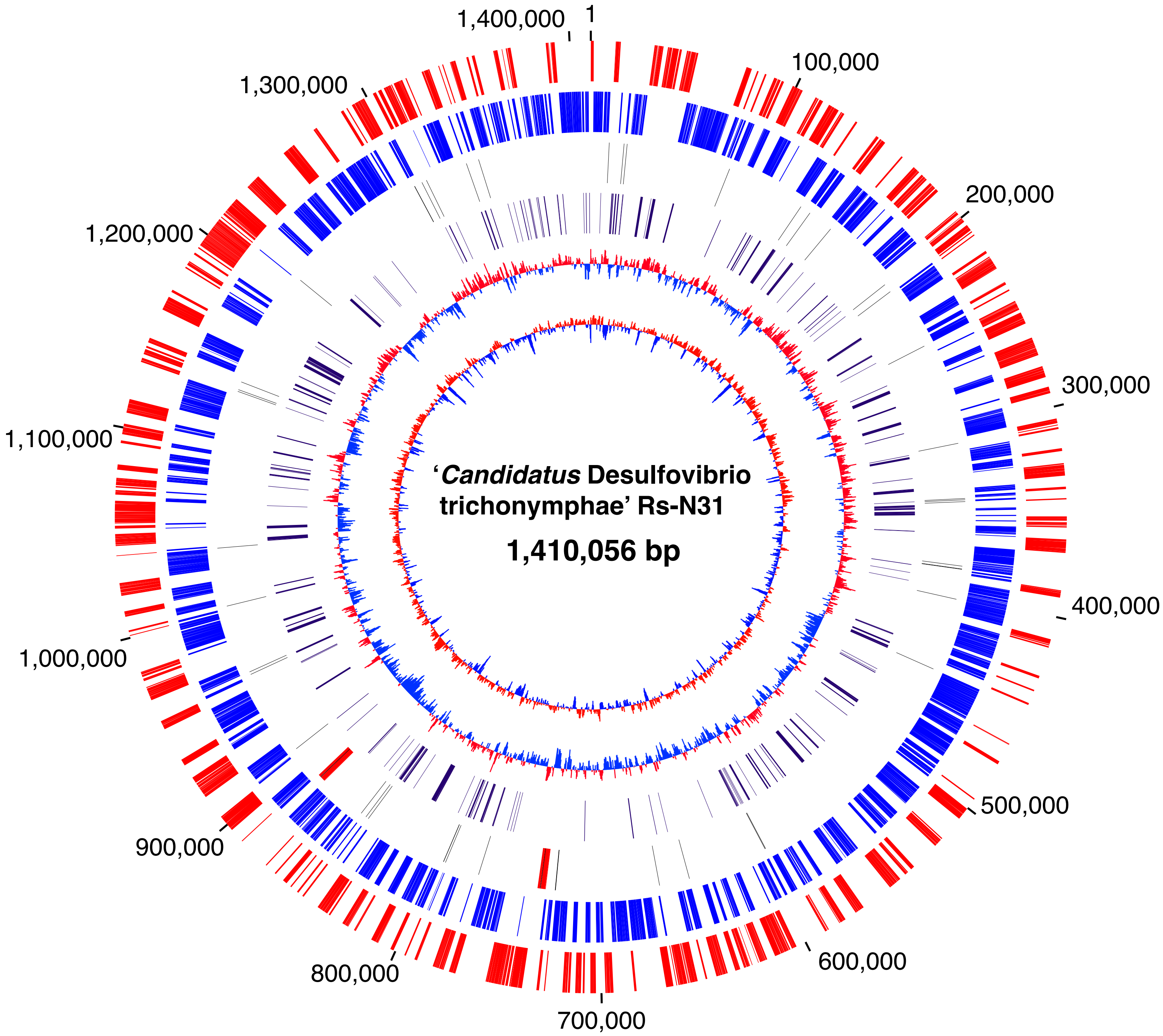

Supplementary Figure S2. Circular representation of the chromosome of '*Ca*. Desulfovibrio trichonymphae' phylotype Rs-N31. The concentric rings denote the following features (from outside): (1) CDSs present on the forward strand, (2) CDSs present on the reverse strand, (3) RNA genes (red: rRNAs), (4) pseudogenes, (5) G + C skew, and (6) G + C content.

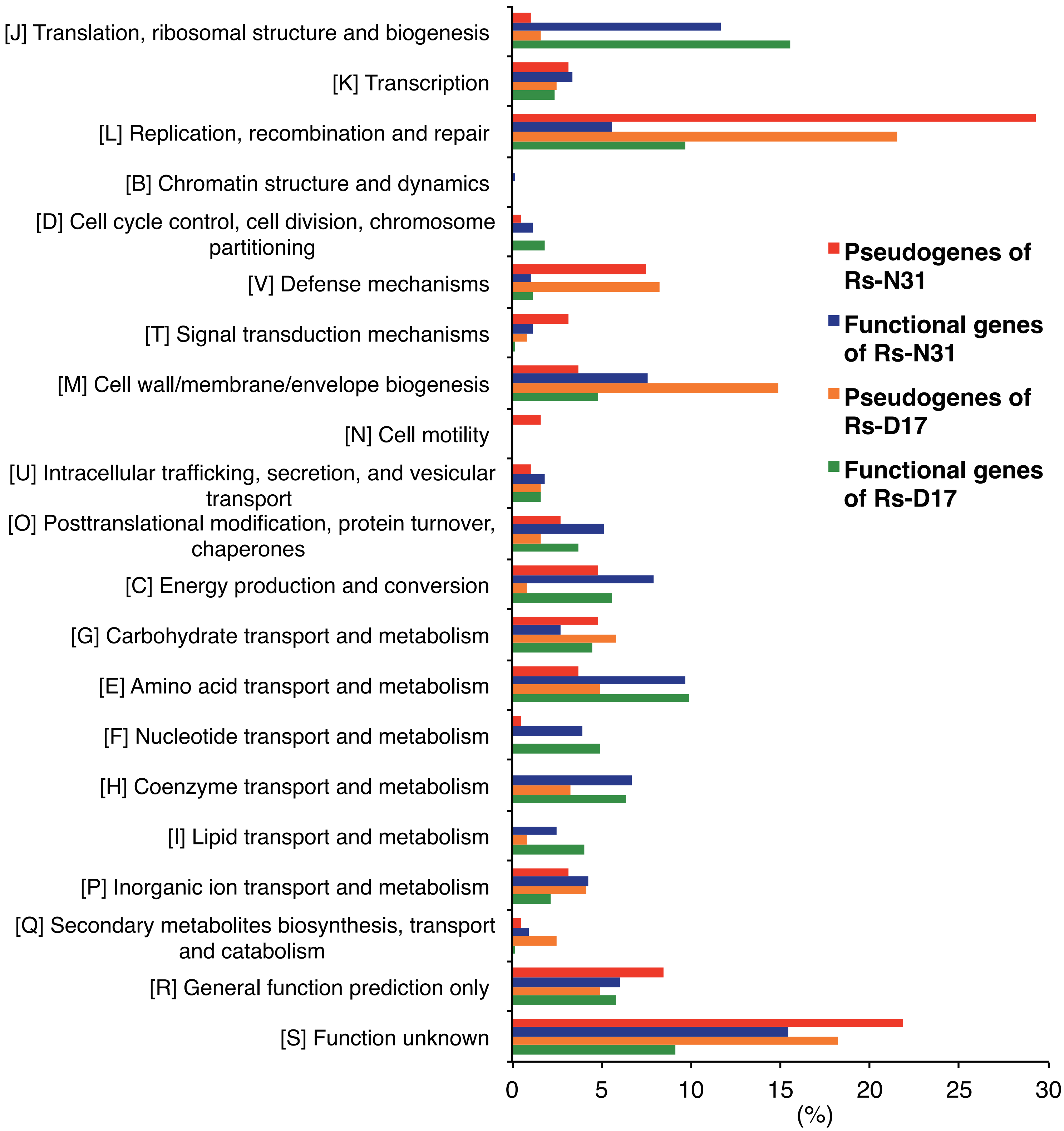

Supplementary Figure S3. Non-supervised orthologous groups (NOG) classification of functional genes and pseudogenes of ‘*Candidatus* Desulfovibrio trichonymphae’ phylotype Rs-N31 and ‘*Candidatus* Endomicrobium trichonymphae’ phylotype Rs-D17.

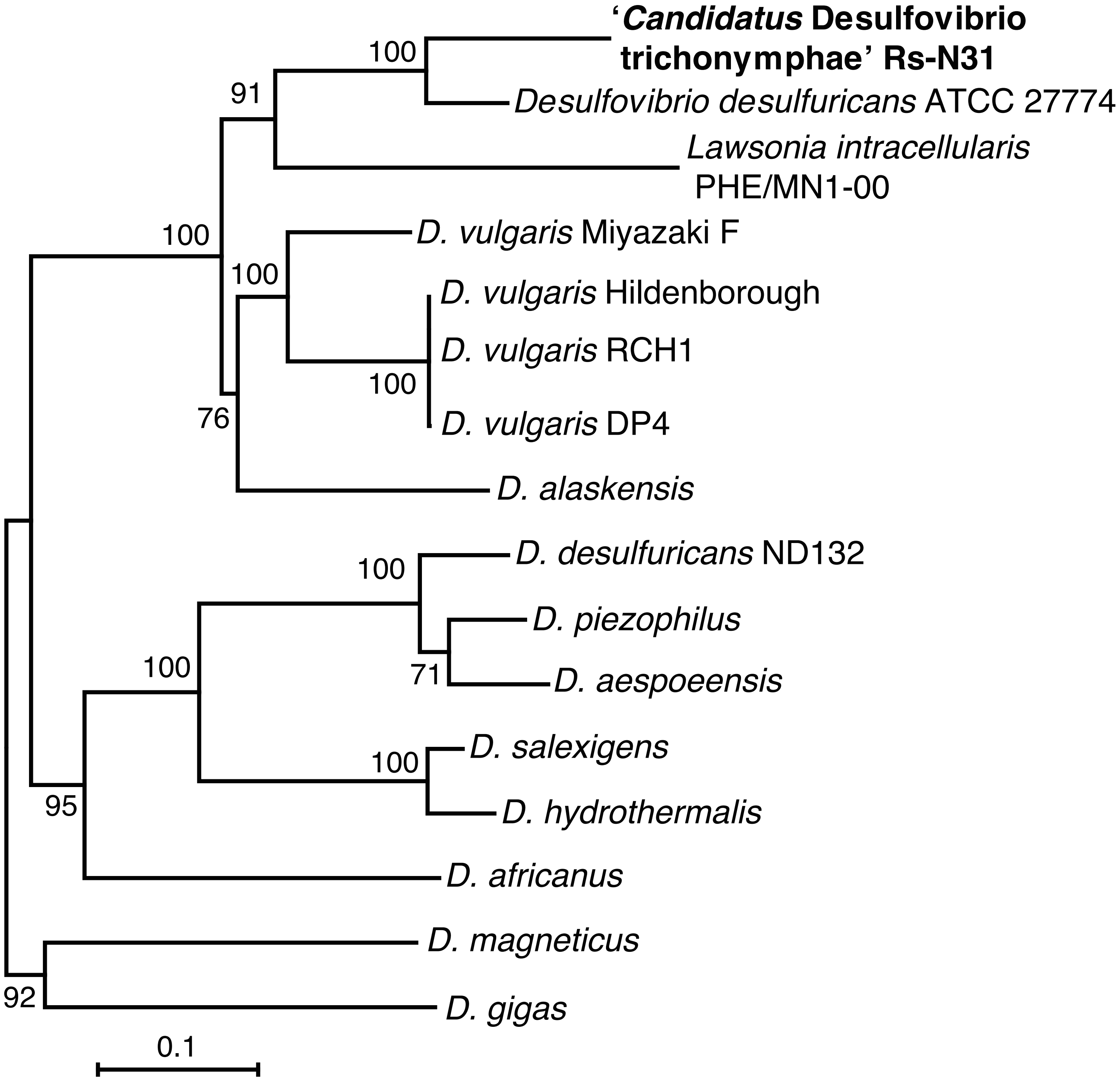

Supplementary Figure S4. Maximum-likelihood tree based on a concatenated amino acid sequence of 30 ribosomal proteins. Ribosomal proteins, L1, L2, L4, L5, L6, L10, L11, L13, L14, L15, L16, L18, L22, L23, L24, L25, L29, S2, S3, S5, S7, S8, S9, S10, S11, S12, S13, S15, S17, and S19 were used. A total of 4,305 aligned amino acid sites were used in the analysis. The LG + Γ + I amino acid substitution model was used. Bootstrap analysis was performed with 500 resamplings.

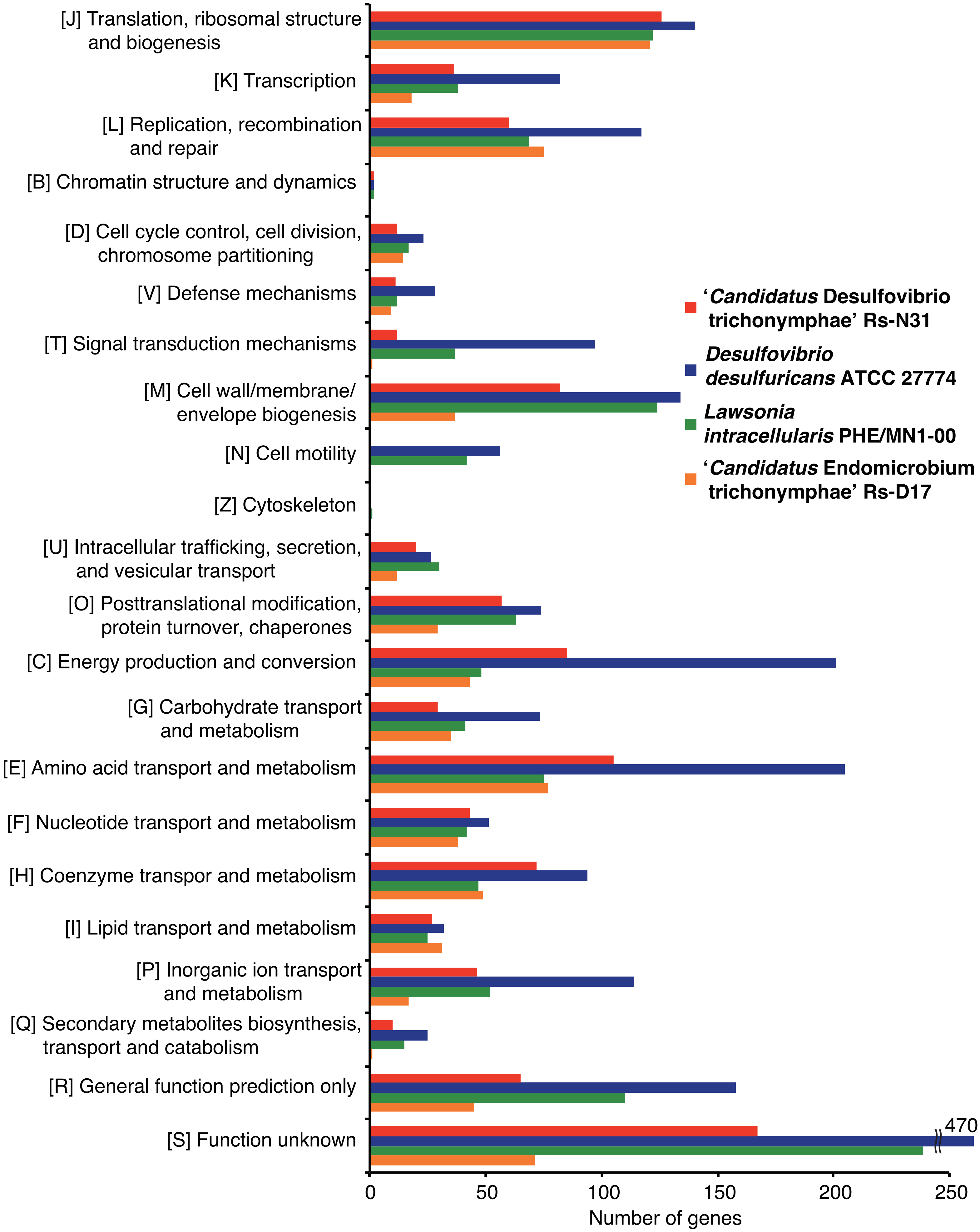

Supplementary Figure S5. Non-supervised orthologous groups (NOG) classification of genes in the genomes of '*Ca*. Desulfovibrio trichonymphae' phylotype Rs-N31 and reference organisms.

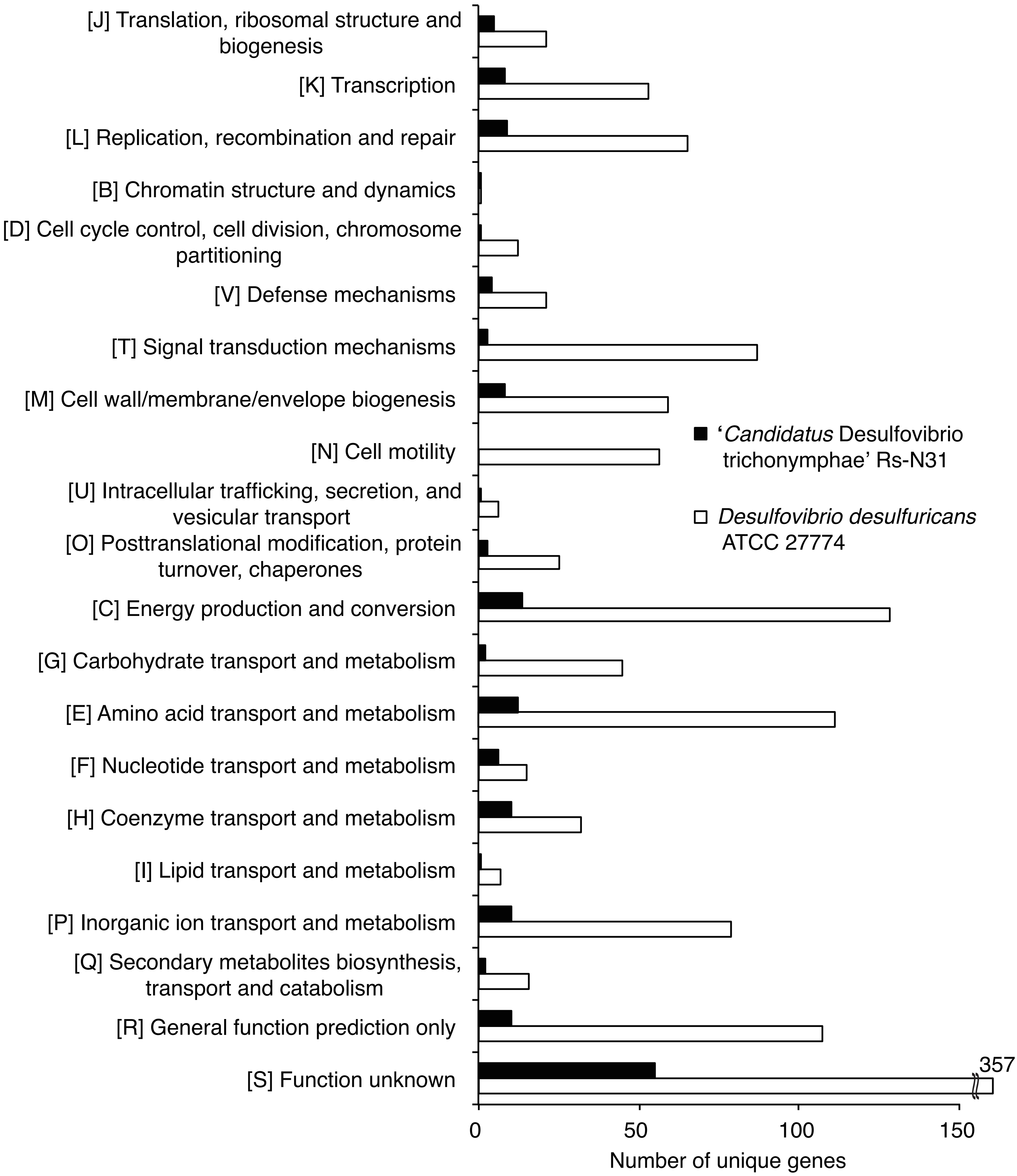

Supplementary Figure S6. Non-supervised orthologous groups (NOG) classification of unique genes between '*Candidatus* Desulfovibrio trichonymphae' phylotype Rs-N31 and *Desulfovibrio desulfuricans* ATCC 27774.

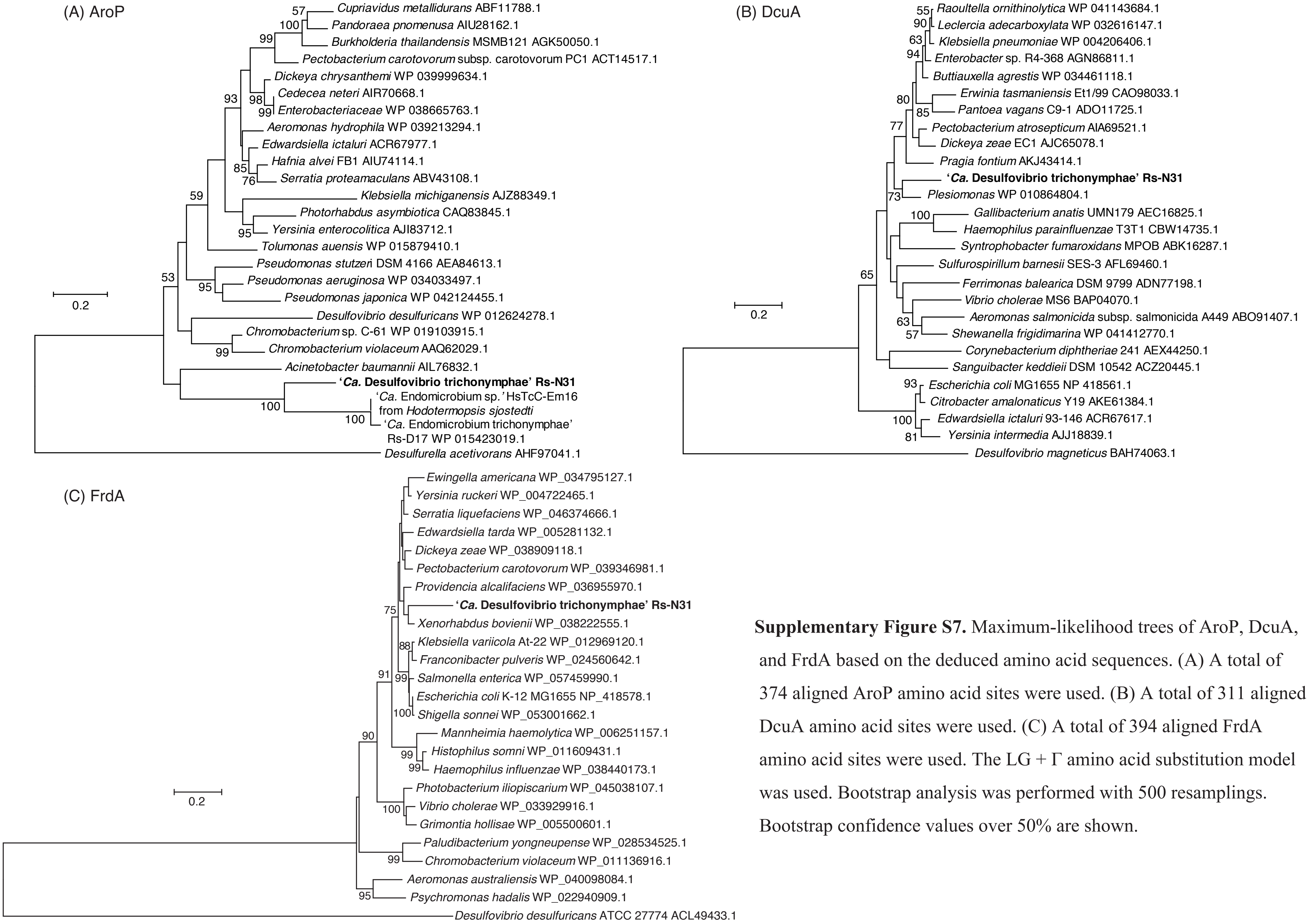

Supplementary Figure S7. Maximum-likelihood trees of AroP, DcuA, and FrdA based on the deduced amino acid sequences. (A) A total of 374 aligned AroP amino acid sites were used. (B) A total of 311 aligned DcuA amino acid sites were used. (C) A total of 394 aligned FrdA amino acid sites were used. The LG + Γ amino acid substitution model was used. Bootstrap analysis was performed with 500 resamplings. Bootstrap confidence values over 50% are shown.

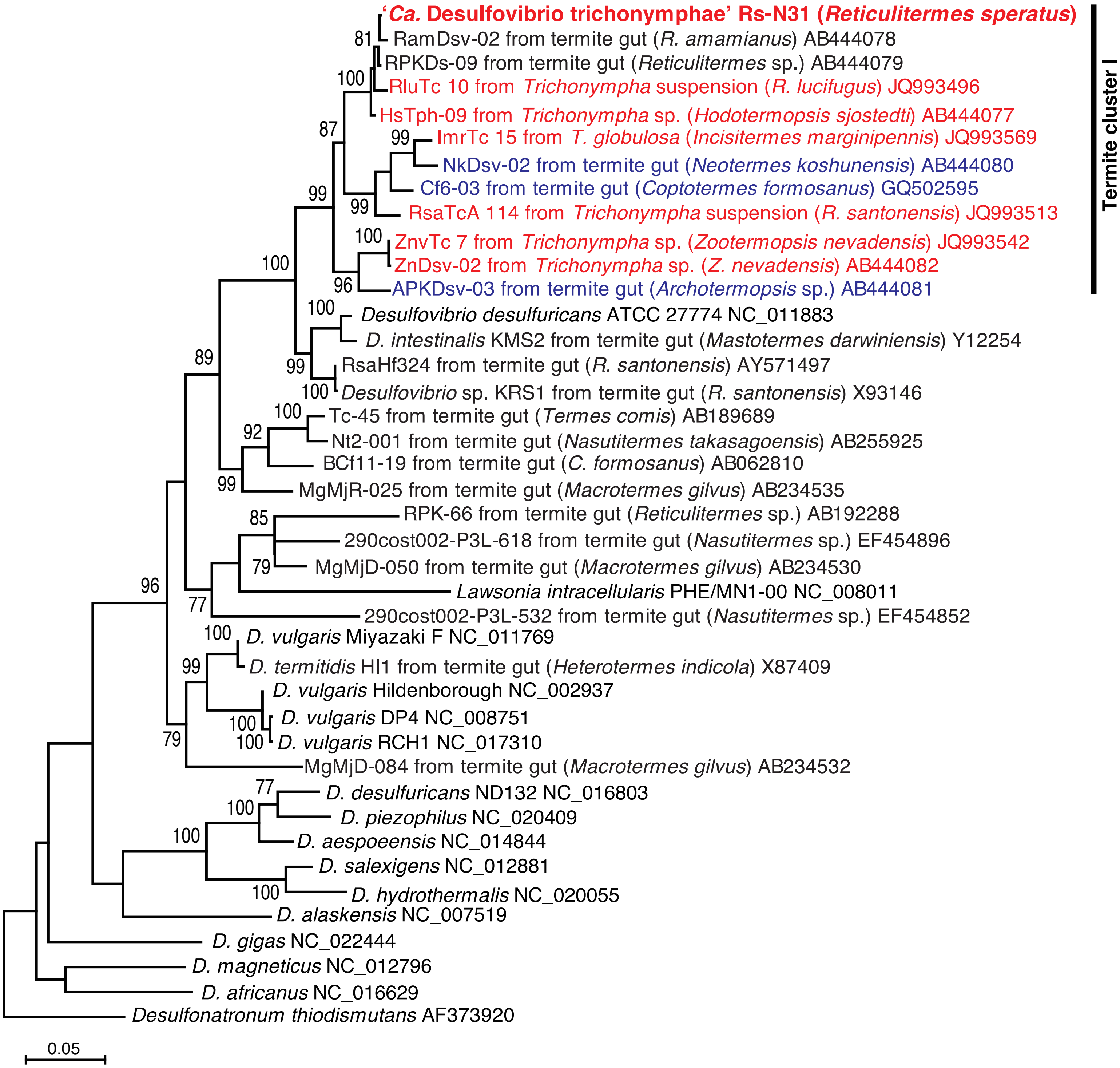

Supplementary Figure S8. Phylogenetic position of '*Candidatus* Desulfovibrio trichonymphae' phylotype Rs-N31 based on the 16S rRNA gene sequence. A maximum-likelihood tree was constructed with a GTR + Γ base substitution model. A total of 1,163 aligned nucleotides sites were used in the analysis.

Bootstrap analysis was performed with 500 resamplings. Bootstrap confidence values over 70% are shown.

Red denotes sequences obtained from *Trichonympha* cells, while blue denotes those from termites that do not harbor *Trichonympha* protists (Strassert *et al*., 2012).